


Antimicrobial performance and instrumental analysis for hexagonal ZnO NPs biosynthesized via *Ziziphus* leaf extract

Rafal Al-Assaly¹, Saba Abdulmunem Habeeb², Asmaa H. Hammadi³, Lena Fadhil Al-Jibouri⁴, Rusul Hameed⁴, Amer Al-Nafiey ^{5,*}

¹Department of Clinical Laboratory Sciences, College of Pharmacy, University of Babylon, Al Najaf's St., Al Hillah, Babil Governorate, 51002, Iraq

²Department of Pharmaceutical Chemistry, College of Pharmacy, University of Babylon, Al Najaf's St., Al Hillah, Babil Governorate, 51002, Iraq

³Department of Pharmaceutics, College of Pharmacy, University of Babylon, Al Najaf's St., Al Hillah, Babil Governorate, 51002, Iraq

⁴Department of Pharmacology and Toxicology, College of Pharmacy, University of Babylon, Al Najaf's St., Al Hillah, Babil Governorate, 51002, Iraq

⁵Department of Laser Physics, College of Science for Women, University of Babylon, Al Najaf's St., Al Hillah, Babil Governorate, 51002, Iraq

*Corresponding author. Department of Laser Physics, College of Science for Women, University of Babylon, Al Najaf's St., Al Hillah, Babil Governorate, 51002, Iraq. E-mail: amer76z@yahoo.com; wsci.amer.khzaer@uobabylon.edu.iq

Abstract

In this study, ZnO (NPs) were successfully biosynthesized using $\text{Zn}(\text{NO}_3)_2 \cdot 6\text{H}_2\text{O}$ as the Zn^{+2} source and fresh *Ziziphus* leaf extract as the reductive and stabilizer reagent. The pH and temperature of the reaction were controlled, and the NPs were calcinated at 500°C for 2 h to produce ZnO. FESEM, EDX, XRD, UV-visible, and FTIR were used to analyze ZnO NPs. UV-Vis spectroscopy confirmed the interaction of the biomolecule with the Zn precursors ($\lambda_{\text{max}} = 362 \text{ nm}$). FESEM revealed hexagonal NPs with a size of 41.7 nm. XRD analysis confirmed a hexagonal structure with an average particle size of 17.4 nm. In addition to this work, we use the Minimum Inhibitory Concentration MIC method using a Biotek 800ST plate reader (Biotek, USA) to examine the antimicrobial efficacy of biosynthesized nanoparticles against standard and clinical strains of *Pseudomonas aeruginosa* (ATCC PAO1), *Streptococcus pneumoniae* (ATCC BAA-334), and local isolate *Candida albicans*. The results of MIC explain that MIC value $125 \mu\text{g/ml}$ with $\text{IC}_{50} = 56.2 \mu\text{g/ml}$ for *Pseudomonas aeruginosa* (ATCC PAO1), MIC value $125 \mu\text{g/ml}$ and $\text{IC}_{50} = 38.9 \mu\text{g/ml}$ for *Streptococcus pneumoniae* (ATCC BAA-334) and MIC value $250 \mu\text{g/ml}$ with $\text{IC}_{50} = 79.3 \mu\text{g/ml}$ for the local isolate *Candida albicans*. This green approach offers a potential strategy for developing eco-friendly antimicrobial agents.

Keywords: biosynthesis; zinc oxide nanoparticles (ZnO NPs); *Ziziphus* leaf extract; antimicrobial activity; characterization techniques; minimum inhibitory concentration (MIC)

Introduction

The field of nanotechnology has garnered significant interest as a potentially effective means of investigating novel antimicrobial drugs to counteract the escalating problem of antibiotic resistance [1, 2]. Designing, characterizing, producing, and applying materials and devices at the nanoscale typically, between (1 and 100) nanometers is the focus of nanotechnology. Because of their small size, nanoparticles have special characteristics such as more controllable and varied applications and enhanced interactions with cells due to their larger surface area-to-mass ratio [3, 4]. The development of devices and structures from different materials is beneficial [5]. Nanometers that are frequently employed in medical applications [6], environmental protection, sunscreen, and cosmetic technology are called nanoparticles [7, 8].

In recent times, there has been an increasing emphasis on developing methodologies for synthesizing nanoscale semiconductors due to their distinct characteristics, rendering them highly suitable for various applications, especially in optoelectronic systems. Presently, within the group of semiconductor materials

documented [9, 10]. ZnO NPs stands out as an inorganic semiconductor exhibiting three distinct crystal lattice structures: rock salts, zinc blends, and wurtzite. The wurtzite configuration is deemed thermodynamically stable at normal room temperature, where each zinc atom is coordinated tetrahedrally with four oxygen atoms [11]. ZnO NPs, which has a broad band gap of 3.1–3.3 eV, has many potential uses in a variety of industries, including antibacterial agents, cosmetics, drug carriers, and biosensors [12]. Several methodologies, including sol-gel processing, homogeneous precipitation, mechanical milling, microwave synthesis, spray pyrolysis, thermal evaporation, and mechanochemical synthesis, can be utilized for the production of ZnO NPs [13]. However, these methodologies typically involve the utilization of perilous reducing agents and organic solvents, the majority of which exhibit high reactivity and are deleterious to the ecosystem. Consequently, the adoption of green synthesis methodologies has been employed in the production of ZnO NPs in an attempt to mitigate environmental repercussions. The methodology known as “green synthesis” harnesses the capabilities of plants and microbes to fabricate nanoparticles with potential

Received: 30 July 2024. Revised: 30 August 2024. Accepted: 11 September 2024

© The Author(s) 2024. Published by Oxford University Press.

This is an Open Access article distributed under the terms of the Creative Commons Attribution License (<https://creativecommons.org/licenses/by/4.0/>), which permits unrestricted reuse, distribution, and reproduction in any medium, provided the original work is properly cited.

applications in the field of biomedicine. A multitude of advantages associated with this approach encompass aspects such as safety, biocompatibility, cost efficiency, and ecological sustainability. Moreover, various studies have illustrated the robust antibacterial properties of ZnO NPs that are manufactured through green synthesis techniques [14].

The green synthesis methods of NPs using plants and microbes have been taken a great interest in the green nanotechnology era, because not only less hazardous chemicals are expected to be used in the process, it is also more cost-effective than the conventional methods of NPs synthesis. The green approach to nanoparticle preparation has numerous advantages because it is compatible with biomedical, drug delivery, imaging, and pharmaceutical applications due to the absence of toxic chemicals, and the nanoparticles formed have controlled shape, size, and stability over physical and chemical approaches. Among the biological resources-mediated synthesis of NPs, microbes have taken a special place in the synthesis process due to their easiness, eco-friendly, and least disturbances of the natural biological diversity [9].

The green technique, which uses plants and is safe, nontoxic, and environmentally beneficial, is becoming popular [15]. Certain nanoparticles, such as titanium dioxide, iron oxide, and zinc oxide, selectively kill cancer cells and can be applied in the treatment of cancer [16]. ZnO NPs were prepared using more environmentally friendly methods, which focused on substituting safer extracts of various natural materials, including bacteria, fungi, plants, and algae, for more hazardous traditional chemicals. The results were ZnO NPs with higher and comparable activities to the traditional ones. For instance, plant extracts from a variety of plants, including *Ganoderma lucidum* [17], *Abelmoschus esculentus* (okra) mucilage [18], *Cuminum cyminum* (cumin) [19], *Azadirachta indica* (Neem) leaf [20], *Calotropis gigantea* leaves [21], *Mangifera indica* (mango) leaves [22], *Cyanometra ramiflora* leaves [23], *Aloe socotrina* leaf [24], and *Ziziphus jujube* (Sidr or Nabq) [25], where the plant extracts are used as stabilizing and capping agents to prevent the production of ZnO NPs. Figure 1, illustrated primary metabolite and general mechanism steps for biosynthesized ZnO NPs used plant extracts.

Ziziphus within the Rhamnaceae family. Also referred to as wild *jujube*, small-fruited *jujube*, the plant is utilized in traditional

medicine to alleviate pain and inflammatory-related illnesses and bioactive metabolites that plants generate [26]. *Ziziphus jujube* is a widely utilized plant with several health advantages that is found in Saudi Arabia and the neighboring areas [25]. A number of long-chain organic compounds, including alpha-tocopherol, beta-carotene, phenolic compounds, flavonoids, sterols, tannins, alkaloids, saponin, and fatty acids, have been found to be abundant in the extract of the *Ziziphus jujube* plant. These compounds may function as capping agents and prevent the agglomeration of nanoparticles (NPs) because they are long-chain natural products [17, 25].

Additionally, environmentally green produced zinc oxide nanoparticles were employed in drug delivery, biomedical applications, and for antioxidant, antibacterial, and anticancer objectives [26, 27]. Numerous studies have demonstrated the effective antibacterial properties of ZnO NPs against various pathogenic bacteria, thus positioning them as viable options for diverse medical purposes. Among the array of biosynthetic methods available, the use of plant extracts in green synthesis has emerged as a particularly promising approach [28]. These nanomaterials, synthesized through green routes, exhibit unique characteristics during their utilization across different sectors, resulting in their widespread application in pharmaceuticals and medical fields. Interest in the exploration of the antibacterial capabilities of metal oxide nanoparticles has recently grown, aiming to develop potent antibacterial agents. The presence of phytochemical nanocomposites surrounding nanoparticles synthesized through green methods enhances their attraction to receptors on the bacterial cell wall, thus boosting their antibacterial efficacy [29]. The bactericidal impact of ZnO NPs, synthesized through green processes, is notable against a broad range of pathogenic bacteria. ZnO NPs, known for their biocompatibility, low toxicity, and expansive specific surface area, have been utilized to impede bacterial growth in various fields such as food packaging, cosmetics, and agricultural disease control [28, 29]. Table 1 listed therapeutic benefits of ZnO NPs and a comparison with other metal and metal oxide NPs that biosynthesized using various plant extracts.

The objective of this study was to produce zinc oxide nanoparticles through an eco-friendly method utilizing organic extracts derived from *Ziziphus* plant leaves. The realization involved the characterization of the nanoparticles via different

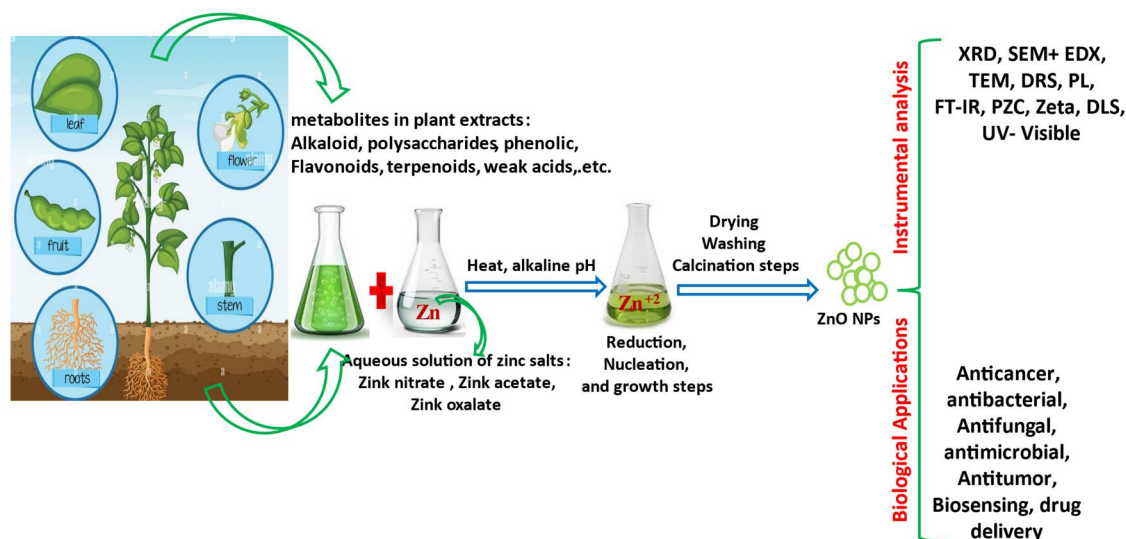


Figure 1. Primary metabolite and mechanism steps of ZnO NPs generation based on plant extracts.

Table 1. Comparative list of metal and oxide metal biosynthesis using various plant extracts based to phytochemicals, metabolites

Metal and metal oxide	Plant extract	Phytochemicals, metabolites, and active groups in plant extract	Instrumental analysis	Therapeutic benefits and applications	References
Zinc oxide (ZnO)	<i>Ziziphus</i>	Alcohols, phenols, carbohydrates, glycosidic, amino acids	FE-SEM + EDX, XRD, FT-IR, UV-visible	Antimicrobial	Present this study
Zinc oxide (ZnO)	<i>Cymbopogon citratus</i>	Polyphenols, tannins, alkaloids, steroids glycosides, saponins, oils, proteins, fats and carbohydrates	HR-TEM, XRD, UV-visible, DLS, EDX, Zeta	Antimicrobial	[30]
Zinc oxide (ZnO)	<i>Abelmoschus esculentus</i>	Carbohydrates	FE-SEM, XRD, FT-IR, UV-visible, Raman	Dye removal	[18]
Zinc oxide (ZnO)	<i>Azadirachta indica</i>	Organic acid, Flavone, Quinone, Aldehyde, Ketone, protein	TEM + EDX, XRD, FT-IR, UV-visible	antibacterial and photocatalytic	[20]
Zinc oxide (ZnO)	<i>Calotropis gigantea</i>	Carboxylic groups	FE-SEM + EDX, XRD, UV-visible, DLS, AFM	tree seedling growth	[21]
Zinc oxide (ZnO)	<i>Cyanometra ramiflora</i>	Phenolic compounds, amines	FE-SEM + EDX, XRD, UV-visible, BET, FT-IR	photocatalytic	[23]
Zinc oxide (ZnO)	<i>Aloe socotrina</i>	Amines groups	SEM, TEM, XRD, UV-visible, FT-IR	Drug delivery	[24]
Zinc oxide (ZnO)	<i>Ziziphus jujuba</i>	Phenols, alcohols, carbohydrates, etc.	XRD, FT-IR, TEM	Dry removal	[25]
Zinc oxide (ZnO)	<i>Ziziphus spina-christi</i>	Terpenoids, saponins, flavonoids, and tannins.	SEM, XRD, FT-IR, UV-visible	Antimicrobial	[27]
Zinc oxide (ZnO)	<i>Ziziphus jujuba</i>	Alcohols, phenols, carbohydrates, etc.	FT-IR, XRD, SEM, TEM, N ₂ adsorption, DRS	Dye removal	[31]
Iron oxide (FeO)	<i>Ziziphus mauritiana</i>	Phenols, saponins, flavonoids and tannins	UV-visible, FTIR, XRD, SEM	Antibacterial	[32]
Nikel oxide (NiO)	<i>Ziziphus spina-christi</i>		UV-visible, XRD, FE-SEM	Antioxidant, Protoscolicidal, Hemocompatibility, and Antibacterial	[33]
Cobalt oxide (Co ₃ O ₄)	<i>Ziziphus oenopolia</i>		UV-visible, XRD, FE-SEM, EDX	antibacterial	[26]
Coper oxide (CuO)	<i>Ziziphus Mauritiana</i>	Coumarins, tannins, saponins, flavonoids, and glycosides.	XRD, SEM, EDX, TEM, BET	–	[34]
Coper oxide (CuO)	<i>Zizyphus spina</i>	amine orenone, aromatic ring, in tertiary amides, flavonoids, terpenoids, tannins, and saponins	UV-visible, TEM, XRD,	Antifungal	[35]
Cobalt oxide (Co ₃ O ₄)	<i>Ziziphus Oxyphylla Edgew</i>	Hydroxyl, carbonyl, amide, alcohols, phenols groups	XRD, SEM, FTIR, EDX	antibacterial	[36]
Gold (Au)	<i>Ziziphus</i>		UV-visible, XRD, TGA, SEM, EDX, AFM, DLS, Zeta	Antimicrobial	[37]
Sliver (Ag)	<i>Ziziphus spina-christi</i>	Amide, peptides, cyclopeptide alkaloids, carboxyl groups	UV-visible, TEM, FT-IR	Adsorption pollutants	[38]

methodologies, as well as the estimation of their effectiveness in combating pathogenic bacteria and fungi (Candida).

Chemicals and methods

Ziziphus extract preparation

Fifty grams of best fresh *Ziziphus* leaves were selected and washed with tap water and ultra-distillation water respectively to remove pollutants and dust, after that, the leaves were allowed to dry in the open air without losing their freshness. After adding 0.5 l of

ultra-distillation water, the leaves were mashed using a high-speed blender. The solution was then filtered through several filter sheets to remove the leaf residues from the extract. The extract is a thick dark green solution, devoid of sediment, and keep in refrigerator until usage, as seen in Fig. 2a [39].

Green synthesis of ZnO NPs

Ziziphus solution was then heated on a hot palate for approximately 120 min. Zn(NO₃)₂·6H₂O was added to the hot solution while stirring rapidly and steadily. To keep the media at pH 8, a

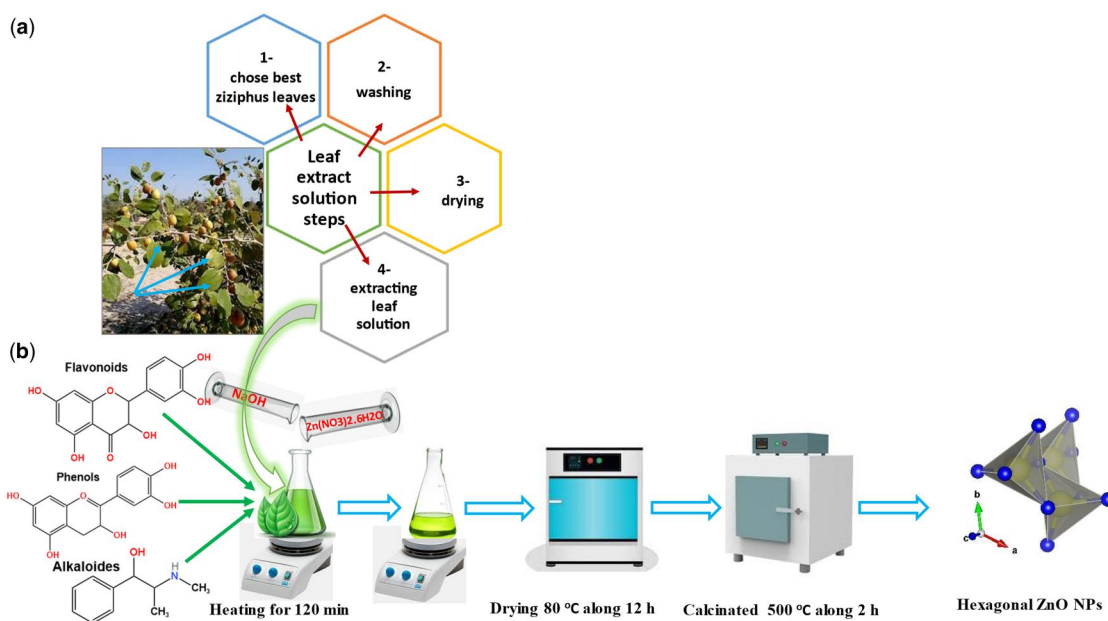


Figure 2. Biosynthesized steps of ZnO NPs used Ziziphus fresh extract. (a) Ziziphus extract, (b) Green Synthesis of ZnO NPs from Ziziphus solution.

few drops of NaOH were added after the Zn(NO₃)₂·6H₂O had dissolved entirely. Stirring the mixture at ambient temperature for approximately 8 h caused the greenish liquid to gradually diminish, revealing a yellow-colored suspension and eventually a pale-yellow precipitate. To remove insoluble Zn(NO₃)₂·6H₂O and other contaminants, the precipitate was washed with tap water and ethanol after being collected via filter paper. Following a 12 h drying period at 80°C, the precipitate was calcined for 2 h at 500°C, showed in Fig. 2b [40].

Analysis of ZnO NPs

KBr pellets were utilized to encapsulate the powder samples for analysis via an FT-IR spectrometer (MAGNA-560) to capture Fourier transform infrared (FT-IR) spectra. The X-ray diffractometer employed was a Rigaku D-max C III, utilizing Ni-filtered K α radiation, while XRD patterns were obtained via a Philips XL30 microscope operating at an accelerating voltage of 10kV. The Debye–Scherrer Equation (1) was used to measure the average size of the nanoparticles [41].

$$D = \frac{0.89 \lambda}{\beta \cos \theta} \quad (1)$$

The symbol λ represents the X-ray wavelength, whereas β represents the full width at half maximum intensity (FWHM).

The use of scanning electron microscopy (SEM + EDX) images enhances the quality of observation and estimation of the morphological characteristics and structural attributes of nanocatalysts.

Antimicrobial section

The microbial suspensions of *Pseudomonas aeruginosa* (ATCC PAO1), *Streptococcus pneumoniae* (ATCC BAA-334) and a local isolate of *Candida albicans* were prepared from 10 single colonies of 24 h old MHA. The colonies were transferred to 2 ml sterile water in 10 ml tubes, after which the absorbance at 600 nm (OD₆₀₀) was measured via a Biotek 800ST plate reader (Biotek, USA). Sterile water was added to a final OD₆₀₀ of 0.236, corresponding to McFarland 0.67. The suspension was diluted 100-fold in MHB for

a final suspension of 1 × 10⁶ CFU/ml, and 50 μ l of this suspension was used to inoculate each well except for the plank wells. The IC₅₀ and MIC were determined according to the methods of [30] in triplicate, in addition to positive and negative control wells.

The inhibitory assay was executed in 96-well microtiter plates, with a total volume of 225 μ l, enhanced with nanomaterials to achieve concentrations ranging from 500 to 31 μ g/ml. These microtiter plates were incubated overnight and then examined for minimum inhibitory concentration (MIC), defined as the lowest concentration at which visual growth inhibition was detected [42].

Results and discussion

Instrumental analysis

The morphological features of the ZnO NPs are illustrated in Fig. 3. Figure 3a and b shows typical SEM images of the samples at 500 and 200 nm, respectively. The form and size of the ZnO NPs appear virtually regular; the majority of them have a hexagonal shape with varying depth, with obvious agglomeration. As shown in Fig. 3c, after scanning the SEM image at 200 nm, the particle size was determined via ImageJ software [43].

Figure 3d shows the combined chemical homogeneous distribution image of ZnO NPs at the particle level, showing that Zn (red) and O (dark orange) are distributed evenly chemically, as presented in Fig. 3e and f [44].

Figure 3g, displays the EDX spectrum of the ZnO nanoparticle samples. The labels reveal the ZnO sample's element names and amounts. The sample clearly has Zn and O as its main components, and no other elements were found within the EDX measurement range. The quantity analysis of the ZnO elements revealed that they contained approximately 82% zinc and approximately 18% oxygen. This shows that the ZnO NP that was made is the purest form possible [45].

X-ray diffraction (XRD) analysis was employed to understand the crystal structure and size of the crystallites in the particles. The XRD profile of the ZnO NPs synthesized through biogenic means is shown in Fig. 4. The XRD peaks at $2\theta = 31.7^\circ, 34.6^\circ, 36.3^\circ, 47.5^\circ, 56.6^\circ, 62.8^\circ, 66.5^\circ, 67.8^\circ, 68.9^\circ, 72.5^\circ,$ and 76.9°

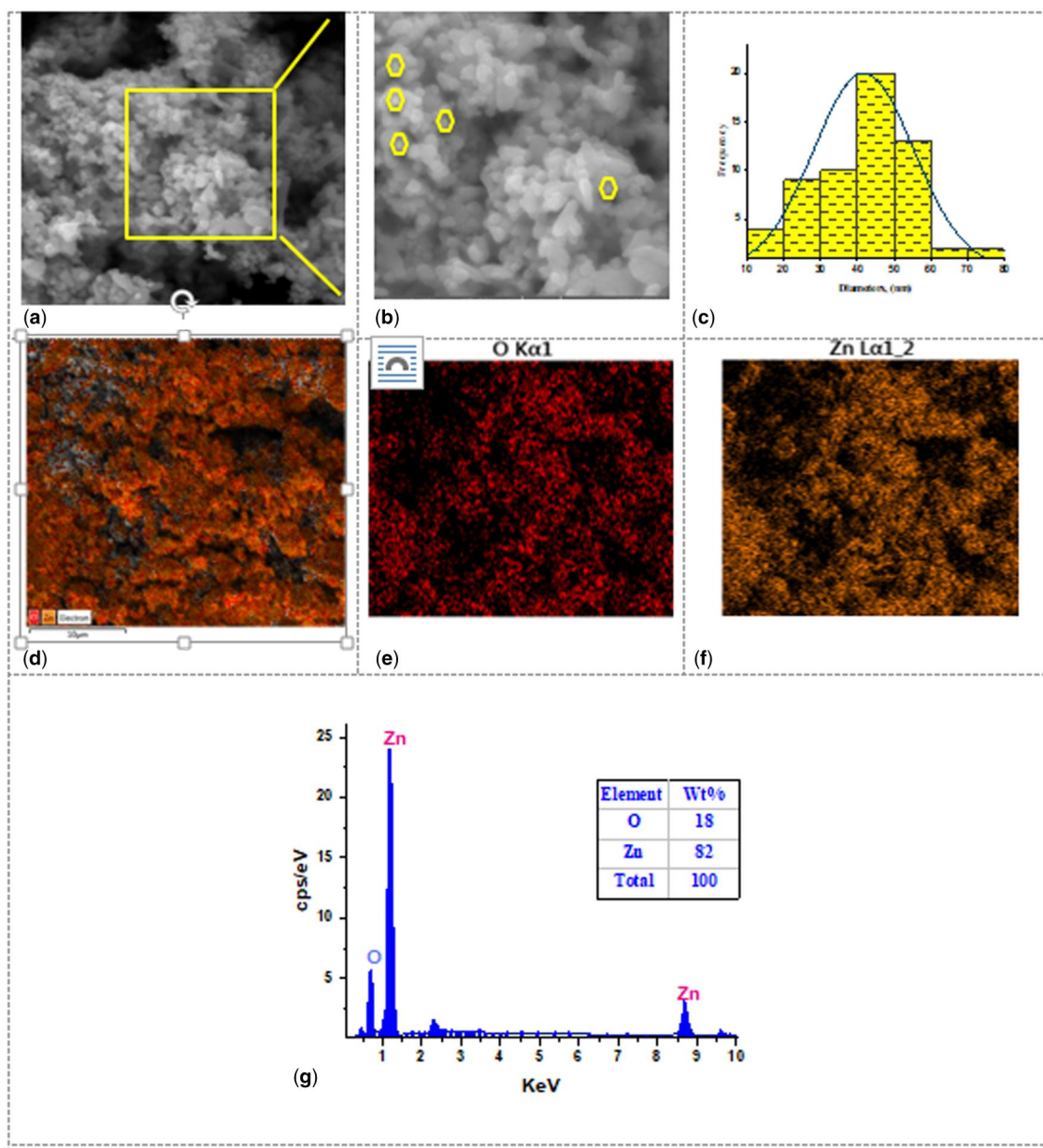


Figure 3. (a and b) FE-SEM images in 500 and 200 nm, (c) histogram distribution of particles, (d–f) elements mapping images, and (g) EDX spectra, for ZnO NPs biosynthesized.

correspond to the (100), (002), (101), (102), (110), (103), (200), (112), (201), (004), and (202) crystal planes, respectively, and the hexagonal crystal geometry corresponds to JCPDS card no. 01-007-2551. The average particle size of the ZnO NPs was found to be approximately 17.4 nm via the “Debye-Scherrer formula” [39].

Figure 5 shows the UV-Vis spectra of the zinc oxide nanoparticles (NPs). The presence of ZnO NPs in the solution is indicated by an absorbance band with a peak at 362 nm. Analysis of the UV-Vis data revealed the absence of an absorption peak at approximately 500 nm, suggesting that the ZnO NPs do not contain ionized oxygen (hydroxyl free). Moreover, the final outcome aligns remarkably well with previously documented studies [45].

FTIR spectroscopy was employed to identify the functional groups present in the ZnO NPs through a green synthesis

approach. The presence of various functional groups in the ZnO NPs is summarized in Fig. 6.

The IR spectra of the synthesized ZnO NPs presented many peaks at 3377, 2151, 1638, 1406, 1364, 1072, 1012, 847, 756, 519 and 453 cm^{-1} . The broad peak at 3377 cm^{-1} indicated the stretching vibration of the O-H group, alcohols, phenols, carbohydrates, and other substances present [46, 47]. The peak at 2150 cm^{-1} corresponds to $\text{C}\equiv\text{C}$ stretching vibrations [48]. The peaks at 1636 and 1410 cm^{-1} are attributed to the $\text{C}=\text{C}$ stretch of alkenes or the $\text{C}=\text{O}$ stretch of amides and the $\text{C}-\text{N}$ stretching bond of an amino acid or may be connect to the water molecule that is adsorbed on the surface [44, 45, 47]. The bands at 1072 and 1012 cm^{-1} correspond to the $\text{C}-\text{O}$ bond of vibration for glycosidic or alcohols or phenols [31]. Furthermore, the peaks at 846 and 756 cm^{-1} may be indicative of amine groups that stretch $\text{C}-\text{N}$ [49]. According to

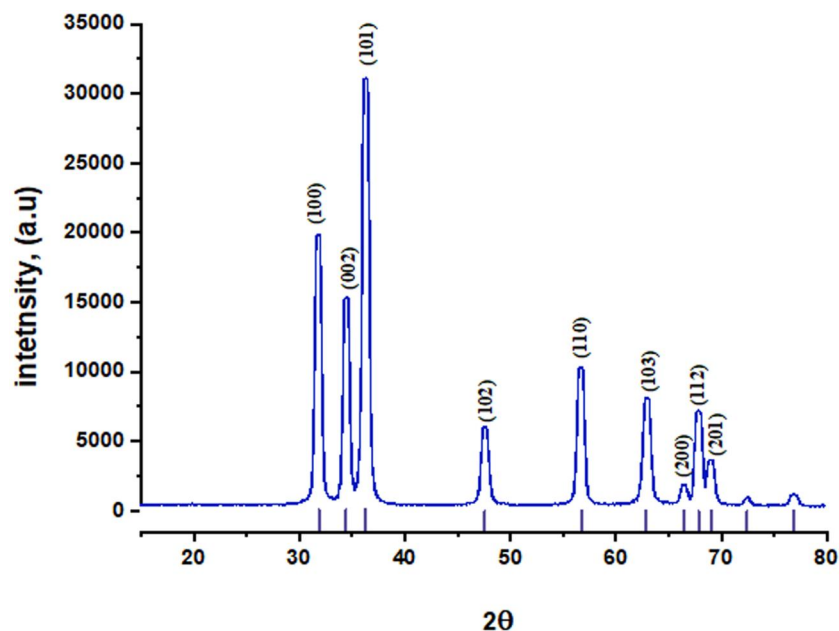


Figure 4. XRD patterns of ZnO NPs.

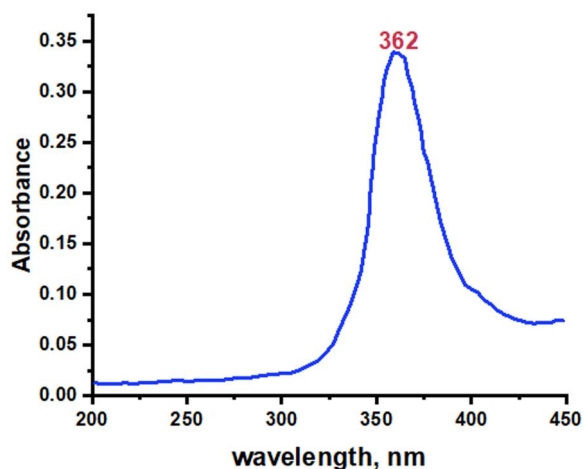


Figure 5. UV-visible analysis of ZnO NPs.

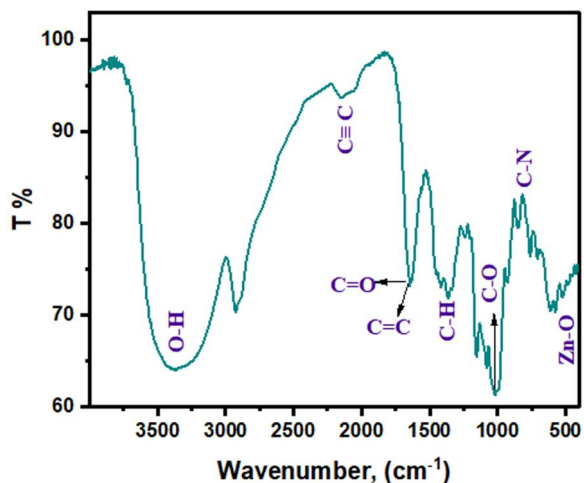


Figure 6. IR spectra for ZnO NPs biosynthesized.

our data, the soft peaks between 453 and 519 cm^{-1} are due to Zn-O stretching bonds. Other researchers have reported similar results [50].

Antimicrobial activity

The efficacy of ZnO NPs as antimicrobial agents targeting both Gram-positive and Gram-negative bacterial strains as well as fungi was assessed through the minimum inhibitory concentration (MIC) methodology. From the Figs 7–12 we noted that the minimum inhibitory concentrations of ZnO NPs against the Gram-negative bacteria *Pseudomonas aeruginosa* and Gram-positive bacteria *Streptococcus pneumoniae* were 125 and $250\text{ }\mu\text{g/ml}$ for *Candida albicans*, with an IC_{50} of $56.2\text{ }\mu\text{g/ml}$, an IC_{50} of $38.9\text{ }\mu\text{g/ml}$ and an IC_{50} of $79.3\text{ }\mu\text{g/ml}$, respectively. The determination of the minimum inhibitory concentration (MIC) is highly important in the context of antibacterial or antifungal utilization. In a manner similar to the current investigation, Gouranga Dutta et al. also fabricated ZnO NPs and silver/zinc oxide Ag/ZnO NPs without subjecting them to subsequent thermal treatment. Additionally, the researchers examined the MIC and MBC of their synthesized materials against Gram-negative and Gram-positive microorganisms, which are very effective against them.

The results of the present study indicate that ZnO NPs are more active against bacteria than fungi and that the effects of ZnO NPs are equal for both gram-positive and gram-negative bacteria, in MIC values with $\text{IC}_{50} = 56.2\text{ }\mu\text{g/ml}$ for *Pseudomonas aeruginosa* and $\text{IC}_{50} = 38.9\text{ }\mu\text{g/ml}$ for *Streptococcus pneumoniae*. The results of this investigation demonstrated the susceptibility of the examined pathogenic strains to ZnO NPs, confirming the potential effectiveness of these nanoparticles against specific bacterial strains. Consequently, there is an opportunity to expand the applications of these NPs within the field of biomedical research [51].

At the past two decades, the drastic evolution in nanotechnology has attracted the attention of various scientific, industrial, agricultural, and biomedical fields to itself. Unique physicochemical properties of these particles including surface potential, high

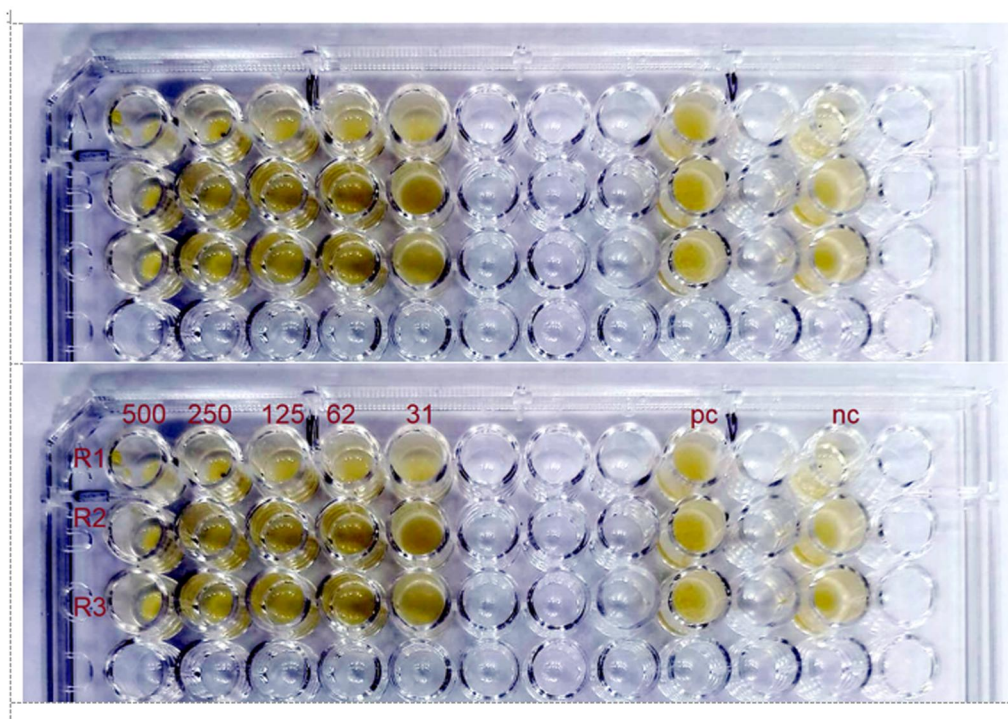


Figure 7. Inhibitory assay for *Pseudomonas aeruginosa*, the microplate represent the treatment of *Pseudomonas aeruginosa* with different concentration, R1, R2 and R3 replica. PC positive control, Nc negative control. MIC value 125 $\mu\text{g/ml}$. IC_{50} = 56.2 $\mu\text{g/ml}$.

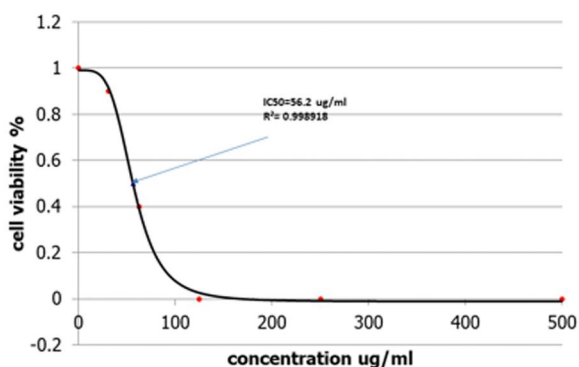


Figure 8. Optical density of cell versus ZnO NPs concentration to calculate IC_{50} .

surface-to-volume ratio, and high reactivity give the opportunity of manufacturing NPs with desired properties and applications. Among NPs, metal/metal-oxide NPs have shown to be more interesting for scientists and engineers and are being widely used in biomedicine and engineering. Some well-known examples of metal-based NPs are gold, copper, iron, silver, aluminum, manganese, and zinc. For metal-oxide NPs, TiO_2 , Al_2O_3 , CuO , CeO_2 , and MnO as individual oxides and LiCoO_2 and BaTiO_2 as binary oxides can be mentioned. These metals possess eccentric physical and chemical properties involving stability, high biocompatibility, and less negative effects on biological systems following large-scale production without making any use of organic solvents. These characteristics define the medical applications of these particles. They can be widely utilized in nanodiagnosis, new drug development, therapy, controlled drug release, drug delivery, and prophylaxis of some kinds of diseases. The mentioned properties are affected and determined by the particles'

size, internal and external shape, chemical composition, structure, etc. [52].

ZnO NPs demonstrate auspicious antibacterial properties, which may be ascribed to their various structural and functional characteristics. Therefore, utilizing leaf extract as a capping agent has the potential to enhance the antibacterial effectiveness of ZnO NPs. Nevertheless, the bactericidal influence of these nanoparticles varies depending on the specific microorganism under scrutiny. Likewise, as Hrishikesh *et al.* pointed out, the findings highlight the significant antibacterial efficacy of ZnO NP-I and ZnO NP-II against *P. aeruginosa* at concentrations of 100, 200, and 500 $\mu\text{g/ml}$ when compared to the control. Particularly, the concentrations of 100 and 200 $\mu\text{g/ml}$ displayed a notably strong antibacterial effect compared to the control throughout the 1st, 2nd, 3rd, 4th, 5th, and 6th hours, thereby validating the present results. By the 24th hour, the increased turbidity of the bacterial culture could be linked to the existence of cellular remnants and noxious substances, resulting in a rise in the opacity of the bacterial culture medium [53].

The antimicrobial characteristics exhibited by ZnO NPs are a result of their interaction with the membrane proteins found in microorganisms. Numerous studies have demonstrated that ZnO NPs have the ability to permeate the cellular membrane of microorganisms and access the internal contents of the cell. A variety of reactive oxygen species (ROS) are subsequently produced, including peroxides (O_2^{2-}), superoxide (O_2^-), hydroperoxyl (HO_2), hydroxyl radical (HO), and singlet oxygen ($^1\text{O}_2$), as well as reactive nitrogen species RNS such as peroxynitrite (ONOO^-) and nitric oxide (NO). Metal and metal oxide NPs can induce ROS bursts by impairing mitochondrial respiration. As an intelligent strategy, metal and metal oxide NPs have been modified by photosensitizers to increase ROS generation. ROS and RNS can lead to protein carbonylation, inactivation of specific enzymes, and lipid peroxidation. It should be regarded that normal amounts of

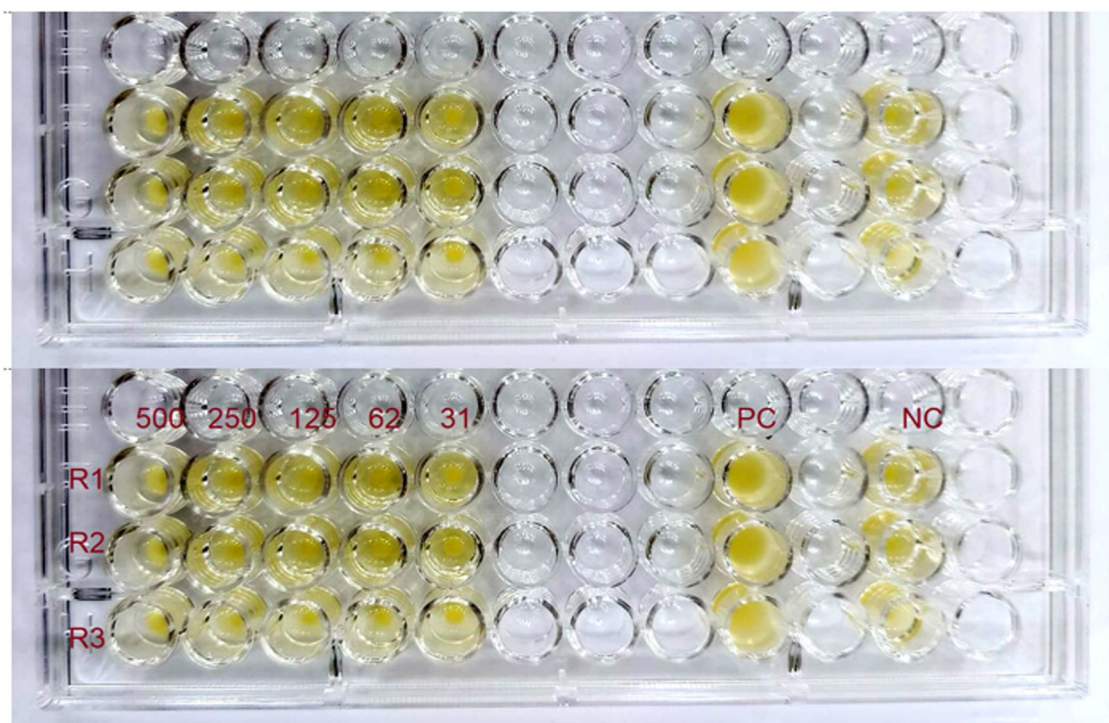


Figure 9. Inhibitory assay for *Streptococcus pneumoniae*, the microplate represent the treatment of *Streptococcus pneumoniae* with different concentration, R1, R2 and R3 replica. PC positive control, Nc negative control MIC value 125 µg/ml. $IC_{50} = 38.9 \mu\text{g/ml}$.

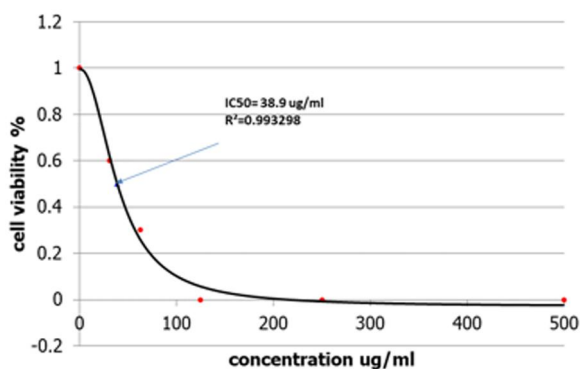


Figure 10. Optical density of cell versus ZnO NPs concentration to calculate IC_{50} .

ROS are generated as a response to the normal metabolisms of oxygen in the body. However, increasing ROS in high concentrations can cause apoptosis and cell death. Therefore, controlling the ROS and RNS in cells is critical to cell survival. Cell survival and cell death are affected by these free radicals or nonradicals such as H_2O_2 . For some metal oxide NPs specifically ZnO NPs, the generation of ROS can be accelerated under visible light and ultraviolet [54]. These ROS inflict damage on vital cellular components such as DNA and proteins, ultimately resulting in the death of the cell [55]. The increased affinity of nanoparticles (NPs) toward cellular membranes could stem from their abundance of positive ions, causing an electrostatic pull toward the negatively charged cell membrane of microorganisms. Consequently, this triggers alterations in morphology, including cytoplasmic contraction, separation of the cell wall, and disruption of the cell membrane. ZnO NPs exhibit effective antimicrobial characteristics, possibly attributed to their distinct structural and functional attributes. However, the bactericidal effects of these nanoparticles

vary depending on the organism examined. A comprehensive understanding of the molecular mechanisms of nanoparticle synthesis can facilitate the manipulation of their antimicrobial activity for the benefit of mankind [29].

Conclusion

In the current investigation, the synthesis of ZnO NPs was successfully achieved using a sustainable method involving the utilization of an aqueous solution containing *Ziziphus* leaf extract as a natural chelating agent responsible for the stabilization of the nanoparticles. FE-SEM, EDX, XRD, UV-visible, and FT-IR techniques were used to study the physical and chemical properties of ZnO NPs. SEM results showed uniformity in shapes and size, with average particle size 41.7 nm. The XRD absorbed the hexagonal phase of ZnO NPs with average particle size of 17.4 nm and high purity. The results of the antimicrobial evaluation demonstrated that the concentration had a significant impact on both bacterial and fungal strains. The results of MIC explain that MIC value 125 µg/ml with $IC_{50} = 56.2 \mu\text{g/ml}$ for *Pseudomonas aeruginosa* (ATCC PAO1), MIC value 125 µg/ml and $IC_{50} = 38.9 \mu\text{g/ml}$ for *Streptococcus pneumoniae* (ATCC BAA-334) and MIC value 250 µg/ml with $IC_{50} = 79.3 \mu\text{g/ml}$ for the local isolate *Candida albicans*. The existence of Zn^{2+} ions initiates enzymatic mechanisms, resulting in the transformation of the hazardous byproduct H_2O_2 into non-toxic substances like oxygen and water. It is important to note that the dimensions, structure, and crystallite size of the particles play pivotal roles in regulating all the observed functions.

Author contributions

Rafal Al-Assaly (Formal analysis [equal], Validation [equal], Writing—original draft [equal]), Saba Abdulmunem Habeeb (Formal analysis [equal], Investigation [equal]), Asmaa H.

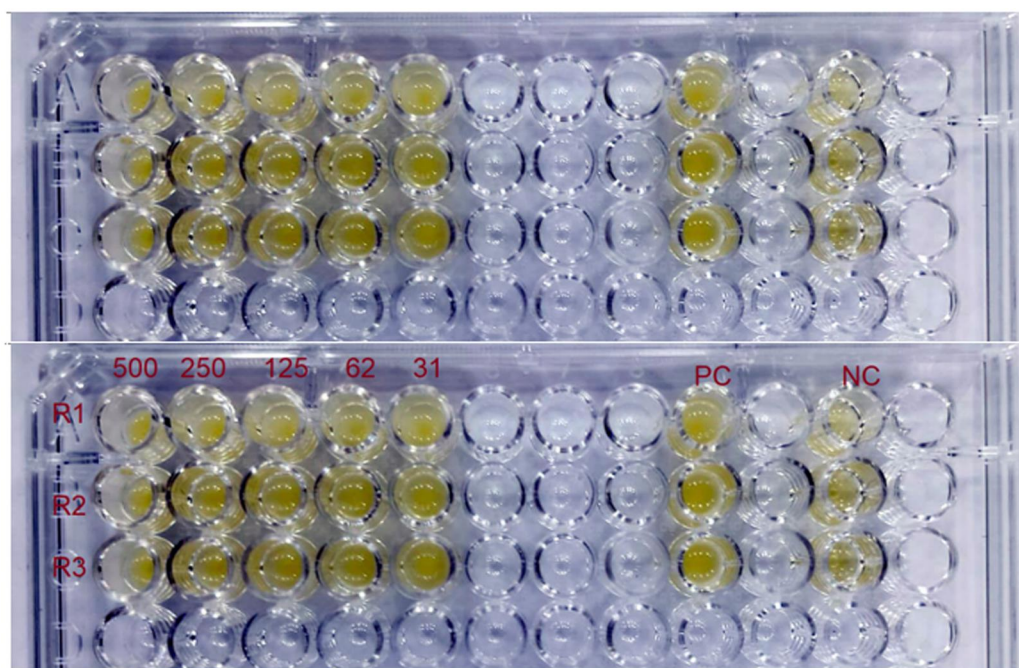


Figure 11. Inhibitory assay for *Candida albicans*, the microplate represents the treatment of *Candida albicans* with different concentration, R1, R2 and R3 replica. PC positive control, Nc negative control MIC value 250 $\mu\text{g/ml}$. IC_{50} = 79.3 $\mu\text{g/ml}$.

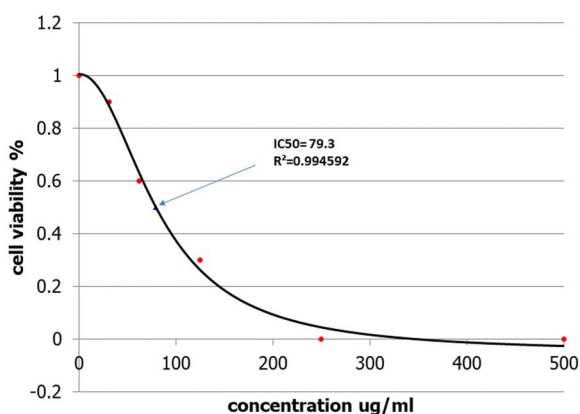


Figure 12. Optical density of cell verses ZnO NPs concentration to calculate IC_{50} .

Hammadi (Investigation [equal], Writing—original draft [equal]), Lena Fadhil Al-Jibouri (Investigation [equal], Methodology [equal], Validation [equal]), Rusul Hameed (Investigation [equal], Methodology [equal]), and Amer Al-Nafey (Project administration [lead], Writing—review & editing [equal])

Conflict of interest: The authors declare that they have no conflicts of interest.

Funding

This research received no external funding.

Data availability

The data that support the findings of this study are available from the corresponding author upon reasonable request.

References

1. Abomuti MA, Danish EY, Firoz A et al. Green synthesis of zinc oxide nanoparticles using salvia officinalis leaf extract and their photocatalytic and antifungal activities. *Biology (Basel)* 2021;**10**. <https://doi.org/10.3390/biology10111075>
2. Björnmalm M, Thurecht KJ, Michael M et al. Bridging bio-nano science and cancer nanomedicine. *ACS Nano* 2017;**11**:9594–613. <https://doi.org/10.1021/acsnano.7b04855>
3. Kaushik NK, Kaushik N, Linh NN et al. Plasma and nanomaterials: fabrication and biomedical applications. *Nanomaterials* 2019;**9**:98–19. <https://doi.org/10.3390/nano9010098>
4. Gold K, Slay B, Knackstedt M et al. Antimicrobial activity of metal and metal-oxide based nanoparticles. *Adv Ther* 2018;**1**: 1–15. <https://doi.org/10.1002/adtp.201700033>
5. Bekele B, Degefa A, Tesgera F et al. Green versus chemical precipitation methods of preparing zinc oxide nanoparticles and investigation of antimicrobial properties. *J Nanomater* 2021;**2021**:1. <https://doi.org/10.1155/2021/9210817>
6. El-Belely EF, Farag MMS, Said HA et al. Green synthesis of zinc oxide nanoparticles (Zno-nps) using arthrospira platensis (class: Cyanophyceae) and evaluation of their biomedical activities. *Nanomaterials* 2021;**11**:95–18. <https://doi.org/10.3390/nano11010095>
7. Mohamad Sukri SNA, Shamel K, Mohamed Isa ED et al. Green synthesis of zinc oxide-based nanomaterials for photocatalytic studies: a mini review. *IOP Conf Ser: Mater Sci Eng* 2021;**1051**: 012083. <https://doi.org/10.1088/1757-899x/1051/1/012083>
8. Nazneen S, Sultana S. Green synthesis and characterization of Cissus quadrangularis. L stem mediated zinc oxide nanoparticles. *Plant Sc Arch* 2024;**9**:1–5.
9. Majeed S, Saravanan M, Danish M et al. Bioengineering of green-synthesized TAT peptide-functionalized silver nanoparticles for apoptotic cell-death mediated therapy of breast adenocarcinoma. *Talanta* 2023;**253**:124026. <https://doi.org/10.1016/j.talanta.2022.124026>

10. Abdel Razzaq A, Al-Nafey A, Al-Marzoqy A. Decorated chitosan with silver-zinc nanoparticles by pulse laser ablation. *Results Opt* 2022;**9**:100282. <https://doi.org/10.1016/j.rio.2022.100282>
11. Doan Thi TU, Nguyen TT, Thi YD et al. Green synthesis of ZnO nanoparticles using orange fruit peel extract for antibacterial activities. *RSC Adv* 2020;**10**:23899–907. <https://doi.org/10.1039/d0ra04926c>
12. Gassim FAZG, Makkawiasmaa Asmaa AJ, Hammadi H. Synthesis and characterization of ZnO-AgCl nanocomposites and applications in the removal of reactive black 5H from wastewater. In: *AIP Conference Proceedings* (Vol. 2547, No. 1). AIP Publishing, 2022.
13. Ahmed Rather G, Nanda A, Ahmad Pandit M et al. Biosynthesis of Zinc oxide nanoparticles using *Bergenia ciliate* aqueous extract and evaluation of their photocatalytic and antioxidant potential. *Inorg Chem Commun* 2021;**134**:109020. <https://doi.org/10.1016/j.inoche.2021.109020>
14. Khan ZUH, Sadiq HM, Shah NS et al. Greener synthesis of zinc oxide nanoparticles using *Trianthema portulacastrum* extract and evaluation of its photocatalytic and biological applications. *J Photochem Photobiol B* 2019;**192**:147–57. <https://doi.org/10.1016/j.jphotobiol.2019.01.013>
15. Bisht G, Rayamajhi S. ZnO nanoparticles: a promising anticancer agent. *Nanobiomedicine (Rij)* 2016;**3**:9. <https://doi.org/10.5772/63437>
16. Vinardell MP, Mitjans M. Antitumor activities of metal oxide nanoparticles. *Nanomaterials (Basel)* 2015;**5**:1004–21. <https://doi.org/10.3390/nano5021004>
17. Alharthi MN, Ismail I, Bellucci S et al. Biosynthesized zinc oxide nanoparticles using *Ziziphus Jujube* plant extract assisted by ultrasonic irradiation and their biological applications. *Separations* 2023;**10**:78. <https://doi.org/10.3390/separations10020078>
18. Prasad AR, Garvasis J, Oruvil SK et al. Bio-inspired green synthesis of zinc oxide nanoparticles using *Abelmoschus esculentus* mucilage and selective degradation of cationic dye pollutants. *J Phys Chem Solids* 2019;**127**:265–74. <https://doi.org/10.1016/j.jpics.2019.01.003>
19. Zare E, Pourseyedi S, Khatami M et al. Simple biosynthesis of zinc oxide nanoparticles using nature's source, and its in vitro bio-activity. *J Mol Struct* 2017;**1146**:96–103. <https://doi.org/10.1016/j.molstruc.2017.05.118>
20. Bhuyan T, Mishra K, Khanuja M et al. Biosynthesis of zinc oxide nanoparticles from *Azadirachta indica* for antibacterial and photocatalytic applications. *Mater Sci Semicond Process* 2015;**32**:55–61. <https://doi.org/10.1016/j.mssp.2014.12.053>
21. Chaudhuri SK, Malodia L. Biosynthesis of zinc oxide nanoparticles using leaf extract of *calotropis gigantea*: characterization and its evaluation on tree seedling growth in nursery stage. *Appl Nanosci* 2017;**7**:501–12. <https://doi.org/10.1007/s13204-017-0586-7>
22. Rajeshkumar S, Kumar SV, Ramaiah A et al. Biosynthesis of zinc oxide nanoparticles using *Mangifera indica* leaves and evaluation of their antioxidant and cytotoxic properties in lung cancer (A549) cells. *Enzyme Microb Technol* 2018;**117**:91–5. <https://doi.org/10.1016/j.enzmictec.2018.06.009>
23. Varadavenkatesan T, Lyubchik E, Pai S et al. Photocatalytic degradation of Rhodamine B by zinc oxide nanoparticles synthesized using the leaf extract of *Cyanometra ramiflora*. *J Photochem Photobiol B* 2019;**199**:111621. <https://doi.org/10.1016/j.jphotobiol.2019.111621>
24. Fahimmunisha BA, Ishwarya R, AlSalhi MS et al. Green fabrication, characterization and antibacterial potential of zinc oxide nanoparticles using *Aloe socotrina* leaf extract: a novel drug delivery approach. *J Drug Deliv Sci Technol* 2019;**55**:101465. <https://doi.org/10.1016/j.jddst.2019.101465>
25. Alharthi MN, Ismail I, Bellucci S et al. Green synthesis of zinc oxide nanoparticles by *Ziziphus jujuba* leaves extract: environmental application, kinetic and thermodynamic studies. *J Phys Chem Solids* 2021;**158**:110237. <https://doi.org/10.1016/j.jpics.2021.110237>
26. Kavica S, Rajesh P, Velmani V et al. Biological synthesis of cobalt oxide nanoparticles using *Ziziphus oenopolia* leaf extract. *J Environ Nanotechnol* 2024;**13**:85–91. <https://doi.org/10.13074/jent.2024.03.241510>
27. Aliyu MS, Shagal MH, Kachalla MR et al. Green synthesis, characterization and antimicrobial activity of zinc oxide nanoparticles from leave extracts of *Ziziphus spina-christi* plant. *Ajstr* 2023;**14**:47–60. <https://doi.org/10.62154/2dvj8172>
28. Matijakovic Mlinarić N, Altenried S, Selmani A et al. Biocompatible polyelectrolyte multilayers with copper oxide and zinc oxide nanoparticles for inhibiting bacterial growth. *ACS Appl Nano Mater* 2024. <https://doi.org/10.1021/acsnm.4c00981>
29. Umavathi S, Mahboob S, Govindarajan M et al. Green synthesis of ZnO nanoparticles for antimicrobial and vegetative growth applications: a novel approach for advancing efficient high quality health care to human wellbeing. *Saudi J Biol Sci* 2021;**28**:1808–15. <https://doi.org/10.1016/j.sjbs.2020.12.025>
30. Abdelbaky AS, Mohamed AMHA, Sharaky M et al. Green approach for the synthesis of ZnO nanoparticles using *Cymbopogon citratus* aqueous leaf extract: characterization and evaluation of their biological activities. *Chem Biol Technol Agric* 2023;**10**:1–23. <https://doi.org/10.1186/s40538-023-00432-5>
31. Alharthi MN, Ismail I, Bellucci S et al. Biosynthesis microwave-assisted of zinc oxide nanoparticles with *Ziziphus jujuba* leaves extract: characterization and photocatalytic application. *Nanomaterials* 2021;**11**:1682. <https://doi.org/10.3390/nano11071682>
32. Karu E, Magaji B, Mohammed Bello A. Green synthesis, spectroscopic analysis and stabilisation energy of iron oxide nanoparticles from aqueous *ziziphus* leaf extract. *Bima J Sci Technol* 2022;**6**:40–49. <https://doi.org/10.56892/bima.v6i03.43>
33. Shnawa BH, Jalil PJ, Hamad SM et al. Antioxidant, protoscolicidal, hemocompatibility, and antibacterial activity of nickel oxide nanoparticles synthesized by *Ziziphus spina-christi*. *BioNanoSci* 2022;**12**:1264–78. <https://doi.org/10.1007/s12668-022-01028-3>
34. Pansambal S, Gonade S, Ghotekar S et al. Green synthesis of CuO nanoparticles using *Ziziphus Mauritiana L.* extract and its characterizations. 2017;**3**:1388–92.
35. El-Abeid SE, Mosa MA, El-Tabakh MAM et al. Antifungal activity of copper oxide nanoparticles derived from *Ziziphus spina* leaf extract against *Fusarium* root rot disease in tomato plants. *J Nanobiotechnol* 2024;**22**:64–24. <https://doi.org/10.1186/s12951-023-02281-8>
36. Saeed SY, Mazhar K, Raees L et al. Green synthesis of cobalt oxide nanoparticles using roots extract of *Ziziphus Oxyphylla* Edegew its characterization and antibacterial activity. *Mater Res Express* 2022;**9**:105001. <https://doi.org/10.1088/2053-1591/ac9350>
37. Aljabali A, Akkam Y, Al Zoubi M et al. Synthesis of gold nanoparticles using leaf extract of *ziziphus zizyphus* and their antimicrobial activity. *Nanomaterials* 2018;**8**:174–15. <https://doi.org/10.3390/nano8030174>
38. Zayed MF, Eisa WH, Abdel-Moneam YK et al. *Ziziphus spina-christi* based bio-synthesis of Ag nanoparticles. *J Ind Eng Chem* 2018;**23**:50–6. <https://doi.org/10.1016/j.jiec.2014.07.041>
39. Habeeb SA, Hammadi AH, Abed D et al. Green synthesis of metronidazole or clindamycin-loaded hexagonal zinc oxide

- nanoparticles from Ziziphus extracts and its antibacterial activity. *Phar* 2022;**69**:855–64. <https://doi.org/10.3897/pharmacia.69.e91057>
40. Hammadi AH, Habeeb SA, Al-Jibouri LF et al. Synthesis, characterization and biological activity of zinc oxide nanoparticles (ZnO NPs). *Syst Rev Pharm* 2020;**11**:431–9. <https://doi.org/10.31838/srp.2020.5.59>.
 41. Habeeb SA, Zinatizadeh AA, Mousavi SA et al. Visible light activated Fe-N-SiO₂/TiO₂ photocatalyst: providing an opportunity for enhanced photocatalytic degradation of antibiotic oxytetracycline in aqueous solution. *IJE* 2023;**36**:615–29. <https://doi.org/10.5829/IJE.2023.36.04A.02>
 42. Ardalani H, Anam S, Kromphardt KJK et al. Coupling microplate-based antibacterial assay with liquid chromatography for high-resolution growth inhibition profiling of crude extracts: Validation and proof-of-concept study with staphylococcus aureus. *Molecules* 2021;**26**:1550. <https://doi.org/10.3390/molecules26061550>
 43. Hammadi AH, Habeeb SA, Al-Jibouri LF et al. Metronidazole-loaded zinc oxide/graphene nanoparticles: synthesis, analysis, drug delivery, and antibacterial efficiency. *Rev Clin Pharmacol Pharmacokinet, Int Ed* 2024;**38**:113–6. <https://doi.org/10.61873/FWIT2515>
 44. Habeeb SA, Zinatizadeh AA, Zangeneh H. Photocatalytic decolorization of direct Red16 from an aqueous solution using B-ZnO/TiO₂ nano photocatalyst: synthesis, characterization, process modeling, and optimization. *Water (Switzerland)* 2023;**15**:1203. <https://doi.org/10.3390/w15061203>
 45. Shnawa BH, Hamad SM, Barzinjy AA et al. Scolicidal activity of biosynthesized zinc oxide nanoparticles by Mentha longifolia L. leaves against Echinococcus granulosus protoscolices. *Emergent Mater* 2022;**5**:683–93. <https://doi.org/10.1007/s42247-021-00264-9>
 46. Shen C, James SA, De Jonge MD et al. Relating cytotoxicity, zinc ions, and reactive oxygen in ZnO nanoparticle-exposed human immune cells. *Toxicol Sci* 2013;**136**:120–30. <https://doi.org/10.1093/toxsci/kft187>
 47. Mozafari MR, Alavi M. Main distinctions between tocosome and nano-liposome as drug delivery systems: A scientific and technical point of view. *Micro Nano Bio Aspects* 2023;**2**:26–29.
 48. Karam ST, Abdulrahman AF. Green synthesis and characterization of ZnO nanoparticles by using thyme plant leaf extract. *Photonics* 2022;**9**:594. <https://doi.org/10.3390/photonics9080594>
 49. Abdelkhalek A, Al-Askar AA. Green synthesized ZnO nanoparticles mediated by Mentha spicata extract induce plant systemic resistance against Tobacco mosaic virus. *Appl Sci* 2020;**10**:5054. <https://doi.org/10.3390/app10155054>
 50. Balogun SW, James OO, Sanusi YK et al. Green synthesis and characterization of zinc oxide nanoparticles using bashful (Mimosa pudica), leaf extract: a precursor for organic electronics applications. *SN Appl Sci* 2020;**2**:1–8. <https://doi.org/10.1007/s42452-020-2127-3>
 51. Ghdeeb NJ, Hussain NA. Antimicrobial activity of ZnO nanoparticles prepared using a green synthesis approach. *Nano Biomed Eng* 2023;**15**:14–20. <https://doi.org/10.26599/NBE.2023.9290003>
 52. Barabadi H, Noqani H, Jounaki K et al. Functionalized bioengineered metal-based nanomaterials for cancer therapy. In: *Functionalized Nanomaterials for Cancer Research*. Academic Press, 2024, 219–260.
 53. Ravichandrika K, Kiranmayi P, Ravikumar RVSSN. Synthesis, characterization and antibacterial activity of ZnO nanoparticles. *Int J Pharm Pharm Sci* 2012;**4**:336–8. <https://doi.org/10.4236/ajps.2018.96094>
 54. Alavi M, Yarani R. Nano micro biosystems ROS and RNS modulation: the main antimicrobial, anticancer, antidiabetic, and antineurodegenerative mechanisms of metal or metal oxide nanoparticles. *Nano Micro Biosyst* 2023;**2023**:22–30.
 55. Dutta G, Kumar Chinnaiyan S, Sugumaran A et al. Sustainable bioactivity enhancement of ZnO-Ag nanoparticles in antimicrobial, antibiofilm, lung cancer, and photocatalytic applications. *RSC Adv* 2023;**13**:26663–82. <https://doi.org/10.1039/d3ra03736c>